

# Generation of axially phase-matched parametric four-wave and six-wave mixing in pure sodium vapor

M. A. Moore, W. R. Garrett, and M. G. Payne

*Chemical Physics Section, Oak Ridge National Laboratory, P.O. Box 2008, Oak Ridge, Tennessee 37831-6378*

(Received 21 July 1988)

Axially propagating phase-matched parametric four-wave and six-wave mixing in pure sodium vapor is an easily documented process that may be confused with other resonant processes such as amplified spontaneous emission or stimulated hyper-Raman emission. We demonstrate and characterize the process in sodium vapor under near-resonant two-photon excitations.

## I. INTRODUCTION

Parametric four-wave mixing (PFWM) processes in pure sodium vapor are well-documented experimental phenomena.<sup>1-6</sup> Significant (PFWM) generation produced by unfocused laser beams requires that the phase mismatch,  $\Delta k$ , between the laser beam and the generated beams be zero. In pure vapors phase matching is usually achieved in PFWM processes by the generated waves propagating at nonzero angles with respect to the incident laser beam. Optimum output is generally achieved at a combination of frequencies and phase matching propagation angles of the generated beams such that the refractive indices and propagation directions produce phase matching while optimizing a combination of resonant enhancement in the nonlinear susceptibility,  $\chi^{(3)}$ , and the overlap of the finite-sized pump and generated beams. Thus PFWM emissions are produced with distributions of frequencies and corresponding conical emission angles that have been well documented experimentally and theoretically by Krasinski *et al.*<sup>4</sup> However, we note that under certain circumstances the dispersive properties of the nonlinear medium are such that phase-matched PFWM can be generated at zero-phase-matching angle to produce axial beams. That is, in addition to the usual process where combined refractive indices and propagation angles produce phase matched generation, it is often possible (particularly in alkali metal vapors) to produce additional coherent four-wave mixing emission where all waves involved in the process travel down the axis of the incident laser beam.

Regular four-wave mixing (FWM) can be produced colinearly with unfocused beams by choosing three input frequencies such that phase matching is achieved without the need of a buffer gas. Bjorklund *et al.*<sup>7</sup> produced axial FWM in pure Na vapor with three input plane waves, and Smith *et al.*<sup>8</sup> made a similar application in Hg vapor. However, in PFWM where two or more of the four waves are generated in the medium,<sup>9</sup> there is less freedom for achieving phase matching since only one frequency is a controlled experimental parameter. Nevertheless, axially propagating PFWM was observed in sodium vapor by Krasinski *et al.*,<sup>4</sup> although the properties of this component were not discussed. In the present instance the PFWM process was observed while studying stimulated hyper-Raman (SHR) emission.<sup>6</sup> Because the axial

PFWM process produces radiation along the laser axis in the forward direction, it mimics amplified spontaneous emission (ASE) and SHR processes in its propagation characteristics. If observed signals are not sufficiently resolved spectrally these processes, which have very different origins, may be confused. This could complicate qualitative and quantitative studies of ASE and SHR phenomena when these processes are produced under circumstances where axially propagating PFWM processes may occur. Indeed recent studies by Moore *et al.*<sup>6</sup> and Garrett *et al.*<sup>10</sup> have shown that, under circumstances where the associated atomic excitation is dipole coupled to the ground state, stimulated hyper-Raman emission occurs only in the backward direction. A number of studies in which the presence of axial PFWM was not recognized, resulted in its interpretation as SHR or ASE processes,<sup>2,11-13</sup> as discussed in some detail by Garrett *et al.*<sup>10</sup>

The four-wave mixing processes of interest in this particular study involve the following: two laser photons, angular frequency  $\omega_L$ , tuned near two-photon resonance with sodium  $3d$  or  $4d$  states; a third photon,  $\omega_3$ , from the virtual  $d$  state to an energy between two lower-lying  $p$  substates (often called the idler photon); and finally, a fourth photon from this level to the  $3s$  ground state [see Figs. 1(a)–1(c)]. The two laser photons and the generated photons satisfy  $2\omega_L = \omega_3 + \omega_4$ . To achieve phase-matched PFWM emission with an unfocused pump beam the propagation vectors of the incident laser and generated waves must satisfy the  $\Delta k = 0$  relation

$$2\mathbf{k}_L = \mathbf{k}_3 + \mathbf{k}_4. \quad (1)$$

This condition guarantees constructive interference of the waves generated in the medium (at  $\omega_3$  and  $\omega_4$ ). The relationship of Eq. (1) is illustrated in Fig. 1(d). The phase-matching angles  $\beta$  and  $\theta$  are conveniently defined in terms of the frequencies involved in the process and the colinear phase mismatch,  $\Delta k_0$ , which is defined as  $\Delta k_0 = k_3 + k_4 - 2k_L$ . Also both angles are always small and, at the relevant frequencies and atomic number densities, the refractive indices  $n(\omega)$  differ only slightly from 1.0. For a particular set of frequencies and corresponding propagation vectors the phase-matching angles may be written, with good approximation, as

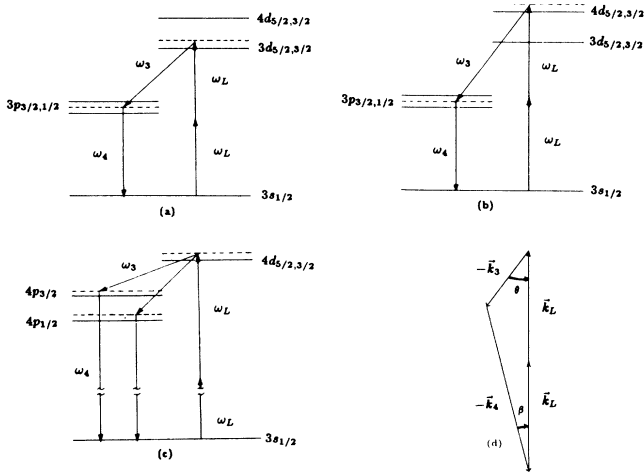


FIG. 1. (a), (b), and (c): Schematic representation of frequencies involved in the axial components of parametric four-wave mixing in pure sodium vapor. Figures are not to scale; (d) phase-matching diagram for PFWM—two laser photons of frequency  $\omega_L$  induce the medium to produce phase-matched radiation at frequencies  $\omega_3$  and  $\omega_4$ .

$$\theta \simeq \left[ \frac{2\Delta k_0}{|\mathbf{k}_3|} \frac{|\mathbf{k}_4|}{|\mathbf{k}_3| + |\mathbf{k}_4|} \right]^{1/2} \simeq \left[ \frac{\Delta k_0}{|\mathbf{k}_3|} \frac{2\omega_L - \omega_3}{\omega_L} \right]^{1/2},$$

$$\beta \simeq \frac{|\mathbf{k}_3|\theta}{|\mathbf{k}_4|} \simeq \frac{\omega_3\theta}{2\omega_L - \omega_3}.$$

To achieve axially phase-matched PFWM emission the propagation vectors must also satisfy

$$2|\mathbf{k}_L| - |\mathbf{k}_3| = |\mathbf{k}_4|. \quad (2)$$

If both Eqs. (1) and (2) are satisfied  $\Delta k = 0$ , and phase-matched PFWM emission can be produced with  $\theta = \beta = 0$ .

The magnitude of the  $k_i$  is  $|k_i| = 2\pi/\lambda_i = \omega_i n(\omega_i)/c$  where  $\omega_i$  is the angular frequency,  $n(\omega_i)$  is the index of refraction at  $\omega_i$ ,  $\lambda_i$  is the wavelength, and  $c$  is the speed of light in vacuum. Within the approximations just noted we can define  $4\pi N\alpha(\omega)/3 = [n(\omega)^2 - 1]/[n(\omega)^2 + 2]$  or  $2\pi N\alpha(\omega) \simeq n(\omega) - 1$ ,<sup>14</sup> where  $\alpha(\omega)$  is the mean microscopic dipole polarizability (essentially real at relevant  $\omega$  values) and  $N$  is the atomic number density of the medium, then Eq. (1.2) may be rewritten as

$$\omega_4\alpha(\omega_4) = 2\omega_L\alpha(\omega_L) - \omega_3\alpha(\omega_3). \quad (3)$$

With reference to the PFWM processes depicted in Fig. 1, note that for frequency  $\omega_4$  the Na vapor exhibits its full range of values of negative and positive dispersion between the fine structure components of the  $p$  states. Thus for the processes shown there is always a spot between the  $p$  substates where axial phase matching may occur regardless of whether the input laser frequency is in a positively or negatively dispersive region. We might also note that the dispersion passes steeply through zero at the exact position of each  $p$  resonance. Thus, over a vanishingly small frequency region, axial phase matching

would appear possible at points near line center of the  $3p_{3/2}$  and  $3p_{1/2}$  resonances. However, the medium absorbs  $\omega_4$  very strongly in these regions. This means that  $\mathbf{k}_4$  becomes complex at these frequencies, and strictly speaking it is then not possible to achieve  $\Delta k = 0$ . The significant damping component remains, and no phase matched generation occurs at the resonant frequencies.

## II. THE EXPERIMENTS

The present observations of axially propagating PFWM processes resulted from monitoring forward and backward emissions from a heat pipe filled with sodium vapor when the incident laser was tuned near two-photon resonance with the  $4d$  state. Sodium pressure was 1.5 Torr and the Lumonics excimer-pumped dye laser had an energy of  $\simeq 5$  mJ/pulse (pulse length = 4 ns). Forward emission in the 5685-Å range (near the wavelength of the  $4d$ - $3p$  transition) was scanned with a Jarrel-Ashe monochromator with a resolving power of 0.3 Å. A spectral scan of the total forward emission is shown in Fig. 2(b) where the pump laser was tuned 0.1 Å to the high-energy side of the  $4d$  levels. Three emission peaks are evident. The outer peaks at 5689.5 Å and 5685.0 Å correspond to the idler wave components,  $\omega_3$ , of conical PFWM generated near the  $4d$ - $3p_{3/2}$  and  $4d$ - $3p_{1/2}$  transition energies, respectively. (The corresponding  $\omega_4$  components at 5891.6 and 5896.5 Å were also observed.) The center peak at 5686.1 Å corresponds to  $\omega_3$  from axially phase-matched PFWM as depicted in Fig. 1(b). The fourth wave in the process (also observed) corresponds to a frequency in the  $3p$ - $3s$  transition range. The emissions were produced only in the forward direction. The corresponding  $\alpha$  for each frequency may easily be calculated under the assumptions that all atoms are in the ground state and that the absorption of nonresonant frequencies is negligible. It was found that Eq. (3) was satisfied within the resolution of the instruments available. For the data shown in Fig. 2(a) a 5-mm aperture was placed in the forward beam that effectively removed most of the familiar conical PFWM emission. As can be seen in the figure, when only axial light is collected the two outer peaks are significantly reduced in intensity.

A similar process is evident when monitoring the axial emission while tuning to two-photon resonance with the  $3d$  state [see Fig. 1(a)] at pressures above 1.5 Torr and at moderately low incident laser intensity (1 mJ/pulse). Results from tuning near the  $3d$  state are shown in (c) and (d) on the right of Fig. 2. The outer peaks are the result of ASE from  $3d$  directly to the  $3p_{1/2}$  or  $3p_{3/2}$  substates. The center peak at 8188.6 Å is the idler component,  $\omega_3$ , from the expected axially phase-matched PFWM process. From a calculation of the appropriate  $\alpha(\omega)$ , it is found that Eq. (3) is again satisfied within the resolution of the experiment. Figure 2(c), right, was taken at a sodium vapor pressure of 2 Torr, while Fig. 2(d), right, was at 3 Torr, both at zero laser detuning from  $3d$  resonance.

Of course this type of emission is not exclusively associated with generation near the  $3p$  states. For example, similar behavior may also be observed in emissions near the  $4p$ - $3s$  states when tuning the dye laser near the two-

photon  $4d$  resonance [see Fig. 1(c)]. In this case the idler frequency,  $\omega_3$ , is in the  $2.3\text{-}\mu\text{m}$  range where our available spectrometers had poor resolving power. Thus we examined instead, the complementary FWM frequency ( $\omega_4$ ) which corresponds to emissions in the  $4p\text{-}3s$  transition region ( $\lambda \approx 3303\text{ \AA}$ ). The uv emission is only evident in the forward direction indicating its origin in FWM rather than ASE. A scan of both the axial and conical forward emissions are shown in Fig. 3(a). An aperture was placed in the forward beam so that only the axial emission is scanned in Fig. 3(b). In Fig. 3(c) a small beam blocking disc was placed in the forward beam to block the axial component and a collecting lens focused the conical emission into the spectrometer. It is evident that there are two axially propagating PFWM signals in this case rather than only one as observed in the  $3d$  case.

We can understand the appearance of two axial PFWM processes associated with the  $4p\text{-}3s$  resonant frequencies if we note the very small magnitude of the oscillator strengths for the  $4p\text{-}3s$  transitions as compared to those for the  $3p\text{-}3s$  transitions (about a factor of 70 smaller). The medium is fairly negatively dispersive at  $\omega_L$  thus the phase-matching frequencies for colinear generation are at points appropriately negatively dispersive at  $\omega_4$ . These are close to the  $4p$  resonances, one at  $\approx 1\text{ cm}^{-1}$  above the  $4p_{1/2}$  resonance, while the second point is  $\approx 2\text{ cm}^{-1}$  to the high-energy side of the  $4p_{3/2}$  sublevel [see Fig. 1(c)]. These points are easily calculated from knowledge of the linear refractive indices. Thus Equation (3) is satisfied at  $3302.22$  and  $3302.91\text{ \AA}$ , while the

resonances are at  $3302.37\text{ \AA}$  and  $3302.98\text{ \AA}$  for the  $4p_{3/2}\text{-}3s_{1/2}$  and  $4p_{1/2}\text{-}3s_{1/2}$  transitions, respectively. Both axial phase-matching points are near, but to the high-energy sides of the fine structure levels. More emission is seen near the  $\frac{3}{2}$  phase-matching point because the oscillator strength for the  $4p_{3/2}\text{-}3s_{1/2}$  transition is twice that for the  $4p_{1/2}\text{-}3s_{1/2}$  transition.

If the oscillator strengths between  $4p$  and  $3s$  states were larger, the phase-matching point above the  $4p_{3/2}$  resonance would move to higher energy, toward the  $4d$  states or if the vapor were less dispersive at  $\omega_L$  the axial phase-matching frequency would be higher (large detuning) and the process would have lower gain. In the case of generation near the  $4d\text{-}3p$  transition the medium is very dispersive at  $\omega_4$ , and the phase-matching point above the  $3p_{3/2}$  level is easily seen to be the trivial solution  $\omega_3 = \omega_4 = \omega_L$ , which lies  $300\text{ cm}^{-1}$  to the high-energy side of the  $3p_{3/2}$  level. However, any axial PFWM signal produced there would be indistinguishable from the incident laser beam. Thus, for the processes studied here it is expected that there will be two axially phase-matched emissions near the  $4p$  resonances, but only one near the  $3p$  resonances.

Hartig<sup>2</sup> also observed four peaks in the forward emissions near the  $4p\text{-}3s$  wavelength range ( $\lambda \approx 3300\text{ \AA}$ ) with better resolution than that of the present study. He attributed two of the four peaks to exact resonant transitions between the  $4p_{3/2}\text{-}3s$  and  $4p_{1/2}\text{-}3s$  states. This conclusion contradicts two important facts. First, there is the lack of any backward uv beam in this frequency region. Resonant processes such as ASE are not unidirectional, but our experiments failed to produce any backward emission in the uv range. Second, if the radiation that Hartig saw was truly resonant, it should have been

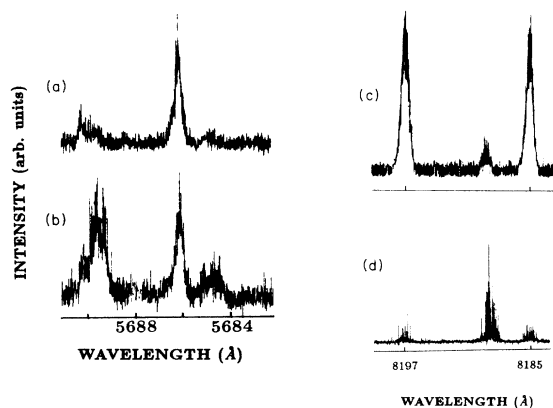


FIG. 2. Left: Profiles of the  $\omega_3$  component (near  $4d\text{-}3p$  transition frequency) of PFWM when tuned near sodium  $4d$  resonance. Upper left (a), axial component only, large peak at  $5686.1\text{ \AA}$  is an axially propagating signal, lower left (b), axial and conical components combined, outer peaks are conically phase-matched PFWM signals from the  $4d\text{-}3p_{3/2}$  ( $5688\text{ \AA}$ ) and  $4d\text{-}3p_{1/2}$  ( $5683\text{ \AA}$ ), respectively.  $P_{\text{Na}} = 1.5\text{ Torr}$ ,  $E = 5\text{ mJ}$  pulse, detuning from two-photon resonance  $\delta = +0.1\text{ \AA}$ . Right: Axial emissions of sodium in the region of  $3d\text{-}3p$  transition when tuned to the two-photon  $3d$  resonance. Sodium pressure  $2\text{ Torr}$ . The outer peaks are  $3d\text{-}3p_{3/2}$  and  $3d\text{-}3p_{1/2}$  ASE, respectively. The center peak at  $8188.6\text{ \AA}$  is the idler frequency,  $\omega_3$ , the axial PFWM process. Sodium vapor pressure is for upper right (c),  $2\text{ Torr}$ , lower right (d),  $3\text{ Torr}$ .

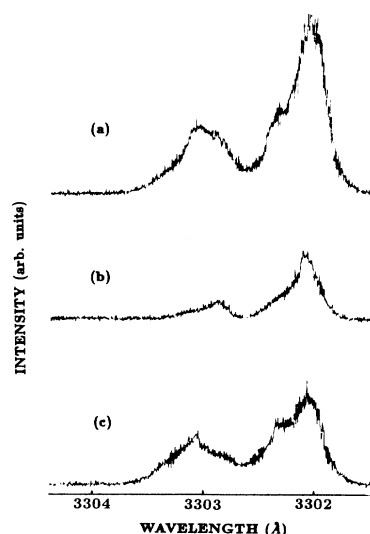


FIG. 3. PFWM signals from two-photon pumping near sodium  $4d$ . These  $\omega_4$  components are near the ultraviolet  $4p\text{-}3s$  transition frequencies. (a) Total forward emission, (b) axial emission only, both peaks due to axial PFWM, (c) conical emission only, four peaks due to conical PFWM.  $P_{\text{Na}} = 0.8\text{ Torr}$ ,  $E = 1\text{ mJ/pulse}$ , detuning from two-photon resonance  $\delta = +0.4\text{ \AA}$ .

so strongly absorbed by the medium as to be essentially unobservable either backward or forward when the number of atoms within the beam significantly exceeds the number of resonant photons. On the basis of the aforementioned processes, Hartig's four peaks probably consisted of emission from the two types of PFWM discussed: two angle-phase matched peaks, positively dispersive at  $\omega_4$ , and two axially phase-matched peaks, negatively dispersive at  $\omega_4$ . His analysis, and those discussed in Ref. 10, reinforce the statement that axial PFWM processes may indeed be mistaken for resonant processes.

Finally we note that phase-matching considerations associated with parametric six-wave mixing (PSWM) are very similar to those of PFWM. Indeed in a process similar to that depicted in the inset in Fig. 4, where two-photon pumping near  $4d$  occurs, PSWM produces emissions near the  $3p_{3/2}-3s_{1/2}$  and  $3p_{1/2}-3s_{1/2}$  wavelengths, in conical distributions qualitatively similar to those observed in PFWM. However, the phase-matching considerations are similar for the four-wave and six-wave mixing processes, thus axial PSWM can occur at a frequency between the two fine-structure levels. Since the medium is negatively dispersive for the laser field, and since the indices for  $\omega_3, \omega_4$ , and  $\omega_5$  are all very near unity, the phase-matching point is in the region above  $3p_{1/2}$  where the medium is negatively dispersive for  $\omega_6$ . In fact the point is essentially where  $2\omega_L \alpha(\omega_L) = \omega_6 \alpha(\omega_6)$ . Upon examination of forward and backward emissions produced when tuning near the  $4d$  state, axially phase-matched parametric six-wave mixing is observed in the forward direction at  $\lambda \approx 8184.6 \text{ \AA}$ , shown in the upper trace in Fig. 4(a). The data were taken with a 5 mm aperture to block conical light from the spectrometer (conically phase matched PSWM emissions at  $\approx 8184$  and  $8195 \text{ \AA}$  are also observed in open geometry). The profile in Fig. 4(a) was taken at  $\delta_L = -0.1 \text{ \AA}$ ,  $P_{Na} = 3 \text{ Torr}$  at  $2.1 \text{ mJ/pulse}$  with an unfocused laser beam. In Fig. 4(b) backward emissions are recorded. As expected the PSWM is not present, but the expected five-photon hyper-Raman emissions at  $8184$  and  $8194 \text{ \AA}$  are seen. Note that the five-photon hyper-Raman emission is not produced in the forward direction due to the accompanying interference from parametric six-wave mixing.<sup>10</sup> This and other features of the hyper-Raman process have been discussed by the authors in separate studies.<sup>6,10</sup>

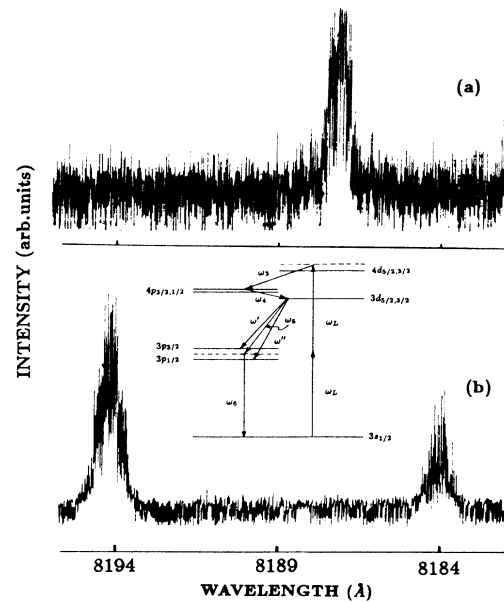


FIG. 4. Inset—depiction of parametric six-wave mixing (PSWM) and five-photon hyper-Raman processes. (a) Forward directed axially phase-matched PSWM ( $\omega_5$  shown, both  $\omega_5$  and  $\omega_6$  observed). (b) Backward propagating five-photon hyper-Raman emissions associated with excitation of  $3p_{1/2}$  and  $3p_{3/2}$  states.

### III. CONCLUSIONS

In conclusion, phase-matching conditions in PFWM processes need not occur only by angle-matched conical propagation of the generated waves. Under certain conditions of moderately high-laser intensity and high number density, it is possible to generate coherent PFWM emission down the laser axis so that all four waves involved in the process travel down the incident laser axis.

### ACKNOWLEDGMENTS

This study comprises a part of a Ph.D. thesis (M.A.M.) in physics at the University of Tennessee, Knoxville, Tennessee. Research was sponsored by the Office of Health and Environmental Research, U.S. Department of Energy under Contract No. DE-AC05-84OR21400 with the Martin Marietta Energy Systems, Inc.

<sup>1</sup>D. M. Bloom, J. T. Yardley, J. F. Young, and S. E. Harris, Appl. Phys. Lett. **24**, 427 (1974).

<sup>2</sup>W. Hartig, Appl. Phys. **15**, 427 (1978).

<sup>3</sup>H. Scheingraber and C. R. Vidal, IEEE J. Quantum Electron. **QE-19**, 1747 (1983).

<sup>4</sup>J. Krasinski, D. J. Gauthier, M. S. Malcuitt, and R. W. Boyd, Opt. Commun. **54**, 241 (1985).

<sup>5</sup>M. S. Malcuitt, D. J. Gauthier, and R. W. Boyd, Phys. Rev. Lett. **55**, 1086 (1985).

<sup>6</sup>M. A. Moore, W. R. Garrett, and M. G. Payne, Opt. Commun. **68**, 310 (1988).

<sup>7</sup>G. C. Bjorklund, J. E. Bjorkholm, P. F. Liao, and R. H. Storz, Appl. Phys. Lett. **29**, 729 (1976).

<sup>8</sup>A. V. Smith, W. J. Alford, and G. R. Hadley, J. Opt. Soc. Am. **B5**, 1503 (1988).

<sup>9</sup>This distinction between regular FWM and PFWM is similar to that of Y. R. Shen, *The Principles of Nonlinear Optics* (Wiley, New York, 1984), p. 117.

<sup>10</sup>W. R. Garrett, M. A. Moore, M. G. Payne, and R. K. Wunderlich (unpublished).

<sup>11</sup>D. Cotter, D. C. Hanna, W. H. W. Tuttlebee, and M. A. Yuratic, Opt. Commun. **22**, 190 (1977).

<sup>12</sup>J. Reif and H. Walther, Appl. Phys. **15**, 361 (1978).

<sup>13</sup>K. Mori, Y. Yasuda, N. Sokabe, and A. Murai, Opt. Commun. **57**, 418 (1986).

<sup>14</sup>M. Born and E. Wolf, *Principles of Optics*, 5th ed. (Pergamon, Oxford, 1975), p. 93.